Chinese Journal of Natural Medicines

Oroxyloside protects against dextran sulfate sodium–induced colitis by inhibiting ER stress *via* PPAR γ activation

Lei TAO, Renjie DOU, Xueming CHEN, Yu CAO, Zhen DAI, Ziyan HU, Zhi MA, Xiaoming GE, Ling ZHANG, Xiaoping WANG

Citation: Lei TAO, Renjie DOU, Xueming CHEN, Yu CAO, Zhen DAI, Ziyan HU, Zhi MA, Xiaoming GE, Ling ZHANG, Xiaoping WANG, Oroxyloside protects against dextran sulfate sodium–induced colitis by inhibiting ER stress *via* PPAR γ activation, Chinese Journal of Natural Medicines, 2024, 22(4), 307–317. doi: 10.1016/S1875–5364(24)60615–1.

View online: https://doi.org/10.1016/S1875–5364(24)60615–1

Available online at www.sciencedirect.com
ScienceDirect
Chinese Journal of Natural Medicines 2024, **22**(4): 307-317
doi: 10.1016/S1875-5364(24)60615-1
Chinese Journal of Natural Medicines

•Original article•

Oroxyloside protects against dextran sulfate sodium-induced colitis by inhibiting ER stress *via* PPARγ activation

TAO Lei[1Δ*], DOU Renjie[2Δ], CHEN Xueming[2], CAO Yu[1], DAI Zhen[1], HU Ziyan[1], MA Zhi[1], GE Xiaoming[1], ZHANG Ling[1], WANG Xiaoping[2*]

[1] *Nanjing Institute for Food and Drug Control, Nanjing 211198, China;*
[2] *State Key Laboratory of Natural Medicines, School of Basic Medicine and Clinical Pharmacy, China Pharmaceutical University, Nanjing 211198, China*

Available online 20 Mar., 2024

[ABSTRACT] Ulcerative colitis (UC), a prevalent form of inflammatory bowel disease (IBD), may result from immune system dysfunction, leading to the sustained overproduction of reactive oxygen species (ROS) and subsequent cellular oxidative stress damage. Recent studies have identified both peroxisome proliferator-activated receptor-γ (PPARγ) and endoplasmic reticulum (ER) stress as critical targets for the treatment of IBD. Oroxyloside ($C_{22}H_{20}O_{11}$), derived from the root of *Scutellaria baicalensis* Georgi, has traditionally been used in treating inflammatory diseases. In this study, we investigated the molecular mechanisms by which oroxyloside mitigates dextran sulfate sodium (DSS)-induced colitis. We examined the effects of oroxyloside on ROS-mediated ER stress in colitis, including the protein expressions of GRP78, p-PERK, p-eIF2α, ATF4, and CHOP, which are associated with ER stress. The beneficial impact of oroxyloside was reversed by the PPARγ antagonist GW9662 (1 mg·kg^{-1}, i.v.) *in vivo*. Furthermore, oroxyloside decreased pro-inflammatory cytokines and ROS production in both bone marrow-derived macrophages (BMDM) and the mouse macrophage cell line RAW 264.7. However, PPARγ siRNA transfection blocked the anti-inflammatory effect of oroxyloside and even abolished ROS generation and ER stress activation inhibited by oroxyloside *in vitro*. In conclusion, our study demonstrates that oroxyloside ameliorates DSS-induced colitis by inhibiting ER stress *via* PPARγ activation, suggesting that oroxyloside might be a promising effective agent for IBD.

[KEY WORDS] Oroxyloside; ER stress; PPARγ; Colitis
[CLC Number] R965 **[Document code]** A **[Article ID]** 2095-6975(2024)04-0307-11

Introduction

Inflammatory bowel disease (IBD) is a refractory intestinal disease characterized by chronic inflammation, resulting in mucosal erosion and ulcers in sections of the gastrointestinal tract. This disease affects 1.4 million Americans, with a prevalence rate of 396 per 100,000 individuals, and is increasingly prevalent in Asian countries [1, 2]. Worldwide, ulcerative colitis (UC), a type of IBD, affects about 8–12 individuals per 100 000 [3]. There is a critical need to explore effective and safe interventions that can mitigate the adverse effects of conventional treatments for UC from a public health perspective. Research has indicated that endoplasmic reticulum (ER) stress may play a significant role in the development of IBD [4, 5]. The ER is a crucial organelle involved in protein synthesis, folding, and modification. Various stressors can lead to the accumulation of misfolded proteins in the ER, triggering the unfolded protein response (UPR) to help the cell adapt to stress or initiate apoptosis [6, 7]. This response involves the dissociation of misfolded or unfolded proteins from GRP78 and the subsequent activation of three primary ER stress transducers: protein kinase RNA-like endoplasmic reticulum kinase (PERK), activating transcription factor 6 (ATF6), and inositol-requiring enzyme 1α (IRE1α). Activation of PERK leads to the phosphorylation of eIF-2α, facilitating the translation initiation of ATF4 and leading to upregulation of CHOP (GADD153). Persistent ER stress, which may occur in various diseases, leads to apoptosis through

[Received on] 28-Jun.-2023
[Research funding] This work was supported by the Science and Technology Program of State Administration for Market Regulation (No. 2021MK136), the Science and Technology Program of Jiangsu Market Supervision and Administration Bureau (No. KJ2022024), and Jiangsu Postgraduate Research and Practice Innovation Program (No. KYCX22_0794).
[*Corresponding author] E-mail: taoleitata@163.com (TAO Lei); cpuwxp@163.com (WANG Xiaoping)
[Δ]These authors contributed equally to this work.
These authors have no conflict of interest to declare.

the sustained activation of the PERK-CHOP signaling pathway. Moreover, all three popular transducers of UPR are regulated by similar cues and coordinately activated [8-14]. Previous studies have identified ER stress in the intestinal mucosa of patients with IBD, including Crohn's disease (CD) and UC [15-18].

Activation of peroxisome proliferator-activated receptor gamma (PPARγ) is recognized for its protective effects on intestinal tissues against damage from dextran sodium sulfate (DSS), 2,4,6-trinitrobenzene sulfonic acid treatment, or ischemia-reperfusion injury [19-21]. Growing evidence highlights the pivotal role of PPARγ in regulating adipocyte differentiation and enhancing insulin sensitivity. PPARγ agonists have been increasingly utilized to manage conditions associated with endoplasmic reticulum (ER) stress, including major depressive disorder (MDD) [22], atherosclerosis, and obesity [23-26]. The PPARγ system provides protection against multiple triggers of the innate immune response, including tumor necrosis factor-α (TNF-α), interferon-γ (IFN-γ), NF-*κ*B, COX2 as well as IL-1, VCAM and MCP1 [27-29].

Oroxylin A, a flavonoid isolated from *Scutellaria* root, has demonstrated a range of pharmacological properties, including anti-inflammatory and antioxidative effects [30, 31]. In our previous study, oroxyloside, a metabolite of oroxylin A, may attenuate DSS-induced colitis through the activation of PPARγ [32]. In this study, we co-treated the mice with GW9662 (an inhibitor of PPARγ) and pretreated the cells with PPARγ siRNA to confirm the crucial role of PPARγ in countering DSS-induced colitis facilitated by oroxyloside. Additionally, we investigated the underlying anti-inflammatory mechanisms of oroxyloside *via* PPARγ activation. Interestingly, our findings revealed that oroxyloside attenuated DSS-induced colitis by inhibiting ER stress *via* PPARγ activation.

Materials and Methods

Chemical Reagents and Kits

Oroxyloside (OAG, $C_{22}H_{20}O_{11}$, *Mr* = 460.39), purchased from Zelang Pharmaceuticals Corporation (Nanjing, China), and freshly diluted with Dulbecco's Modified Eagle Medium (DMEM, Gibco, Carlsbad, CA) to final concentration for *in vitro* study. In addition, oroxyloside was prepared as intragastric administration (0.5% CMC) for *in vivo* study. The mice in the DSS-treated group were administered 0.5% CMC as a vehicle.

LPS (*E. coli*: Serotype O55:B5), 5-Aminosalicylic acid (5-ASA), Dimethylsulfoxide (DMSO), and GW9662 were bought from Sigma-Aldrich (St. Louis, MO, USA). Dextran sulfate sodium (DSS, molecular weight 36–50 kDa) was obtained from MP Biomedicals Inc. (Irvine, CA, USA). Dye DAPI was purchased from Invitrogen (Carlsbad, CA, USA). Triton X-100 was purchased from Shanghai Chao Rui Biotech. Co., Ltd. (Shanghai, China). BSA was obtained from Roche Diagnosis Ltd. (Shanghai, China). Sodium carboxyl methyl cellulose (CMC) was purchased from Sinopharm Group Co., Ltd. (Shanghai, China).

The myeloperoxidase (MPO) kit and activity assay total antioxidant capacity assay kit were obtained from Nanjing Jiancheng Bioengineering Institute (Nanjing, China). ELISA kits for mouse IL-1β, TNF-α, and IL-6 were purchased from Boster Biotech Co. Ltd. (Wuhan, China).

Primary antibodies against PPARγ, p-eIF2α, ATF4, IL-1β, IL-6, TNF-α, *β*-actin, and PPARγ siRNA (M) were purchased from Santa Cruz Biotechnology (Santa Cruz, CA, USA); primary antibodies against p-PERK, CHOP, and GRP78 were purchased from Cell Signaling Technology (Danvers, MA, USA).

Cell culture

The RAW 264.7 mouse macrophage cells were purchased from the Cell Bank of the Shanghai Institute of Biochemistry & Cell Biology at the Chinese Academy of Sciences (Shanghai, China). These cells were cultured in Dulbecco's Modified Eagle Medium (Gibco, Carlsbad, CA, USA) supplemented with 10% (*V*/*V*) heat-inactivated fetal bovine serum (FBS, Gibco, Paisley, Scotland), 100 $U \cdot mL^{-1}$ streptomycin, and 100 $U \cdot mL^{-1}$ penicillin at 37 °C in an atmosphere containing 5% CO_2. Bone marrow-derived macrophages (BMDM) were isolated from C57BL/6 mice and resuspended in DMEM supplemented with 10% FBS and 20 $ng \cdot mL^{-1}$ granulocyte-macrophage colony-stimulating factor (GM-CSF) (PeproTech, USA). The culture medium was replaced every three days, and within approximately one week, a population of adherent macrophages was established. Following a 6-hour incubation period in medium without GM-CSF, these cells were utilized for experimental purposes as BMDM.

Reactive oxygen species formation assessment

The generation of reactive oxygen species (ROS) was assessed using the fluorescent dye 2,7-dichlorofluorescein-diacetate (DCFHDA, Beyotime Institute of Biotechnology, China). Colonic tissues from mice in each experimental group were homogenated with phosphate-buffered saline (PBS). Both isolated colon cells and RAW 264.7 cells were collected and incubated with 10 $\mu mol \cdot L^{-1}$ DCFH-DA, diluted in serum-free medium for half an hour at 37 °C in the dark. Following incubation, the cells were washed twice with a serum-free culture medium. The fluorescence intensity of DCFH-DA in each group was then measured using a measured by FACSCalibur flow cytometer (Becton Dickinson) at *Ex*/*Em* = 488/525 nm.

DSS-induced colitis and drug administration

Female C57BL/6 mice, aged 6–8 weeks old and weighing 18–22 g, were supplied by Animal Core Facility, Nanjing Medical University, with the animal production number SCXK(SU)2021-0001. All the experiments were approved by the Ethics Committee of China Pharmaceutical University. These experiments adhered to the guidelines of the policies of the State Food and Drug Administration (SFDA) of China on Animal Care. All animals received humane care according to the criteria outlined in the *Guide for the Care and Use of*

Laboratory Animals by the National Academy of Sciences, as published by the National Institutes of Health. Throughout the acclimatization and study periods, all animals had unrestricted access to food and water ad libitum and were maintained under a consistent 12 h light/dark cycle at 21 ± 2 °C and a relative humidity of 45% ± 10%.

To induce acute colitis, C57BL/6 mice were administered drinking water containing 4% (*W*/*V*) DSS (model) for seven days, followed by regular water for three days.

All the mice were randomly allocated into four groups: control (receiving regular water), DSS-treated, oroxyloside-treated (80 mg·kg^{-1}, i.g.), and a group receiving GW9662 (PPARγ antagonist, 1 mg·kg^{-1}, i.p.), followed by oroxyloside treatment (80 mg·kg^{-1}). Oroxyloside and GW9662 were administered daily from day 1 to day 10.

Histological analysis of colonic lesions

Mice were inspected and weighed daily. On the eleventh day, the animals were euthanized, and their colons were removed, unfolded longitudinally for photographic documentation, and rinsed with PBS. Sections of THE colonic tissue were then prepared for *ex vivo* analyses. Histological examinations were conducted following previously described methods [33].

Measurement of total antioxidant capacity of the colonic tissues

Colonic tissues were homogenized in cold PBS. The supernatant from each group was then assessed in accordance with the manufacturer's instructions provided with the assay kit.

Transient Transfection

PPARγ siRNA was transfected into cells using Lipofectamine 2000^{TM} reagent (Invitrogen, CA), according to the manufacturer's instructions [34].

Immunoblotting

Cells were exposed to indicated concentration of oroxyloside for 24 h and then collected and lysed in lysis buffer (100 mmol·L^{-1} Tris-Cl, pH 6.8, 4% (g·L^{-1}) sodium dodecylsulfonate, 20% (*V*/*V*) glycerol, 200 mmol·L^{-1} *β*-mercaptoethanol, 1 mmol·L^{-1} phenylmethylsulfonyl fluoride, and 1 g·mL^{-1} aprotinin). The lysates were centrifuged at 12,000 *g* for 30 min at 4 °C. Protein concentrations were determined using a BCA assay kit. The proteins were then separated on an SDS–PAGE gel and transferred to PVDF membranes (Millipore, Billerica, MA). Detection was carried out with primary antibodies followed by incubation with appropriate secondary antibodies. Immunoreactive protein bands were visualized by an Odyssey Scanning System (Li-COR Inc., Superior St. Lincoln, NE). All blots were stripped and reprobed with a polyclonal anti-*β*-actin antibody to confirm equal loading of proteins.

Immunofluorescence microscopy

Briefly, colonic sections were deparaffinized at 60 °C for 30 min, rehydrated, and washed in 1% PBS Tween for 15 min. Then they were treated with 3% hydrogen peroxide, followed by blocking with 3% bovine serum albumin (BSA). The samples were incubated overnight at 4 °C with primary antibodies against CHOP (diluted at 1 ∶ 80). After three washes, the colonic sections were incubated with FITC-conjugated secondary antibodies (diluted at 1 ∶ 200, Invitrogen, CA, USA, M30101, L42001). Slides were counterstained with DAPI for 30 min to visualize nuclei. The reaction was stopped by thorough washing with water for 5 min. Images were captured using a confocal laser-scanning microscope (Olympus, Tokyo, JP). Settings for image acquisition were identical for control and experimental tissues.

Treated RAW 264.7 cells were harvested and seeded onto glass coverslips processed for immunofluorescence. To investigate the expressions of ER stress-associated proteins GRP78 and CHOP, the cells were transfected with PPARγ siRNA for 6 h or not and then pretreated with LPS (1 μg·mL^{-1}), oroxyloside (100 μmol·L^{-1}) for 24 h and then harvested. Coverslips were fixed in 4% paraformaldehyde (PFA) for 30 min. Then the cells were stained with DAPI for 15 minutes. The images were captured by an Olympus FV1000 confocal microscope.

Enzyme-linked immunoassay (ELISA)

Colonic tissues from mice in each group were homogenized with lysis buffer to extract colonic protein. The homogenate was centrifuged at 12 000 *g* at 4 °C for 25 min. The amount of total extracted protein was determined by the BCA protein assay kit. IL-1β, IL-6, and TNF-α production in supernatant RAW 264.7 cells, BMDM cells and serum of mice were measured by ELISA kits according to the manufacturer's specifications. Additionally, the concentrations of IL-1β, IL-6, and TNF-α in the colon homogenates were measured using an ELISA kit.

Immunohistochemistry (IHC)

The protein expression levels of F4/80, GRP78, and CHOP in the colonic tissues were assessed following the method described in the previous study [35]

Quantitative real-time polymerase chain reaction (PCR) analysis

Total RNA isolation and real-time PCR were performed as previously described [35]. The relative amount of target mRNA was determined using the comparative threshold cycle (C_t) method by normalizing target mRNA C_t values to those for *β*-actin (ΔC_t). The primer sequences are as follows: Mouse IL-6-forward (5'-ACAACCACGGCCTTCCCTAC-3'); Mouse IL-6-reverse (5'-TCTCATTTCCACGATTTCCC-AG-3'); Mouse IL-1β-forward (5'-TGCCACCTTTTGAC-AGTGATG-3'); Mouse IL-1β-reverse (5'-TTCTTGTGAC-CCTGAGCGAC-3'); Mouse TNF-α-forward (5'-ATGAG-CACAGAAAGCATGATCCGC-3'); Mouse TNF-α-reverse (5'-AAAGTAGACCTGCCCGGTC-3'); Mouse CHOP-forward (5'-CTGCCTTTCACCTTGGAGAC-3'); Mouse CHOP-reverse (5'-CGTTTCCTGGGGATGAGATA-3'); Mouse sXBP1-forward (5'-GAGTCCGCAGCAGGTG-3'); Mouse sXBP1-forward (5'-GTGTCAGAGTCCATGGGA-3'); Mouse *β*-actin-forward (5'-AAGATGACCCAGATCATGTTT-GAGACC-3'); Mouse *β*-actin-reverse (5'-AGCCAGTCC-

AGACGCAGGAT-3').

Statistical analysis

The data shown in this study were expressed as means ± SD from at least three independent experiments, with each treatment or dosage tested in triplicate samples. Statistical analyses were performed using ANOVA followed by a post hoc test.

Results

Oroxyloside attenuated inflammatory symptoms of DSS-induced colitis by PPARγ activation

The dextran sulfate sodium (DSS)-induced colitis model is widely recognized as closely relevant to human ulcerative colitis [36]. We investigated the anti-inflammatory effects of oroxyloside on the susceptibility and inflammatory responses in this model. We observed significant body weight loss in mice with DSS-induced colitis. However, administration of oroxyloside (80 mg·kg^{-1}) remarkably reversed the weight loss (Fig. 1A). GW9662, a PPARγ inhibitor, negated the beneficial effect of oroxyloside on body weight in mice with colitis (Fig. 1A). As shown in Figs. 1B and 1C, DSS-induced colon shortening was significantly ameliorated by oroxyloside treatment. This improvement, however, was inhibited by GW9662, suggesting that the protective effects of oroxyloside against DSS-induced colitis are mediated, at least in part, through the activation of PPARγ.

Oroxyloside inhibited the inflammatory cell infiltration in DSS-induced colitis via PPARγ activation

In order to evaluate the protective effect of oroxyloside against DSS-induced colitis *via* PPARγ activation, we conducted histopathological analyses using hematoxylin & eosin (H&E) staining (Fig. 2A). The mucosal damage caused by DSS was characterized by significant ulceration, accompanied by extensive infiltration of granulocytes and mononuclear cells into the mucosa, as well as congestion and edema in the submucosa. The results showed that the mucosal damage in the DSS + GW9662 group was similar to, or even more severe than, that observed in the DSS group, indicating that the protective effect of oroxyloside on pathological damage was negated by the PPARγ inhibitor GW9662. Furthermore, we investigated the effect of oroxyloside on the infiltration of inflammatory cells by identifying F4/80 positive (F4/80$^+$) macrophages in the colonic tissues (Fig. 2B). The presence of F4/80$^+$ cells increased in the colonic tissues of mice treated with DSS and DSS + GW9662, while oroxyloside decreased the F4/80$^+$ cells (shown brown) in mice with colitis (Fig. 2B). However, GW9662 blocked the inhibitory effect of oroxyloside on the infiltration of F4/80$^+$ macrophages in colonic tissues of mice with colitis. Furthermore, we found that oroxyloside suppressed the activity of MPO, a hallmark of neutrophil infiltration [37, 38], in mice with colitis. The inhibitory effect of oroxyloside on the neutrophil infiltration was reversed by GW9662 as well (Fig. 2C). Our data indicated that oroxyloside inhibited the infiltration of inflammatory cells in DSS-induced colitis *via* PPARγ activation.

Oroxyloside diminished pro-inflammatory cytokines of DSS-induced colitis

The secretion of pro-inflammatory mediators is a defining feature of dextran sulfate sodium (DSS)-induced colitis [39, 40]. Our results, as depicted in Figs. 3A and 3B, suggested that the levels of IL-1β, IL-6, and TNF-α in the serum and colon were significantly elevated following DSS treatment, with similar increases observed when DSS was combined with GW9662. Oroxyloside effectively reduced the production of these pro-inflammatory cytokines, but this inhibitory effect was negated by GW9662. Additionally, these results were corroborated at the mRNA level (Fig. 3C), further supporting the conclusion that oroxyloside attenuates the production of pro-inflammatory cytokines in the DSS-induced colitis model through the activation of PPARγ.

Oroxyloside counteracted DSS-induced oxidative stress by PPARγ activation

Mounting evidence suggests that the uncontrolled overproduction of ROS can cause oxidative damage during active episodes of inflammatory bowel disease (IBD), indicating that oxidative stress might contribute to the progression of colonic inflammation [41]. In this study, we determined DSS-induced oxidative stress by detecting the colonic ROS pro-

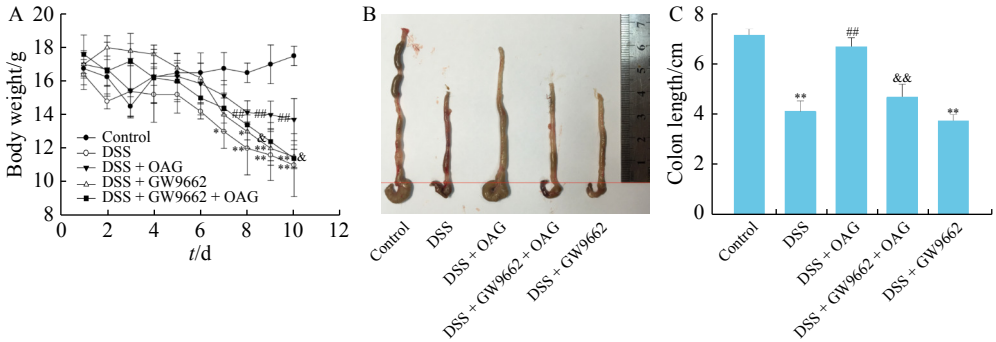

Fig. 1 Oroxyloside treatment attenuated DSS-induced experimental colitis. (A) Body weight changes of each group (n = 10 per group) after DSS induction of colitis. (B, C) The lengths of the colon from each group of mice were measured. The results are representative of three independent experiments and expressed as means ± SD. $^{*}P < 0.05$, $^{**}P < 0.01$ *vs* normal mice; $^{\#\#}P < 0.01$ *vs* DSS-treated colitis mice and $^{\&\&}P < 0.01$ *vs* DSS + OAG-treated colitis mice.

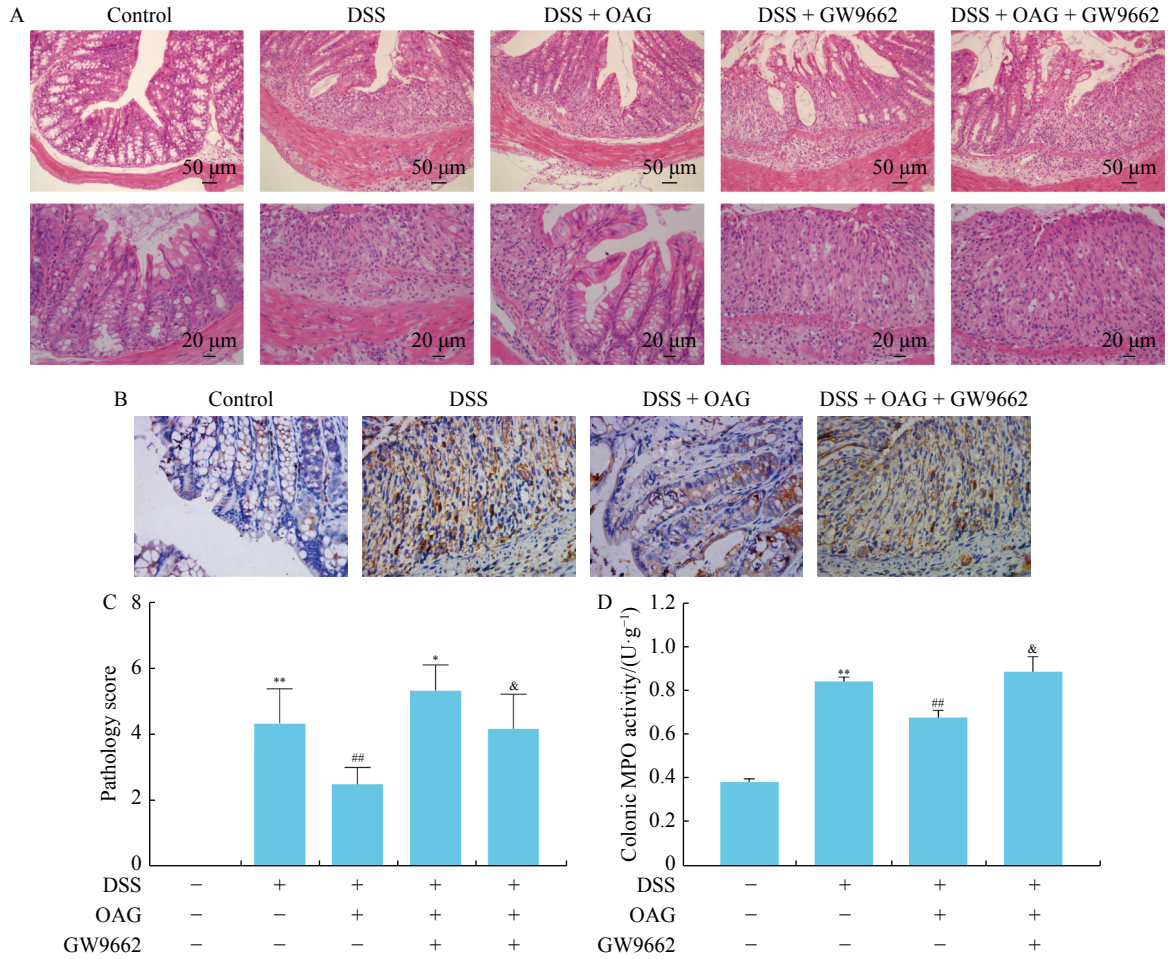

Fig. 2 Oroxyloside prevented DSS-induced colon damage and the infiltration of inflammatory cells in mice with colitis. (A) Serial sections of colonic tissues were stained with H&E (200 ×, 400 ×). (B) The pathology score was performed to evaluate the therapeutic effect of oroxyloside (n = 3 per group). (C) The expression of F4/80$^+$ was detected by IHC (× 400) in colonic tissues, and the positive cells were brown. (D) MPO activities in the colonic tissues were detected (n = 3 per group). The results are expressed as means ± SD. * $P < 0.05$, $^{**}P < 0.01$ *vs* normal mice; $^{\#\#}P < 0.01$ *vs* DSS-treated colitis mice and $^{\&}P < 0.05$ *vs* DSS + OAG-treated colitis mice.

duction and total antioxidant capacity. Notably, as shown in Figs. 4A and 4B, DSS exposure led to an increase in ROS generation in mice with colitis, while oroxyloside treatment effectively reduced this ROS increase. However, the effect of oroxyloside was significantly diminished by GW9662. Furthermore, oroxyloside significantly restored the total antioxidant capacity that was reduced by DSS, and this antioxidative activity of oroxyloside was also negated by GW9662 (Fig. 4C). These findings indicate that oroxyloside mitigates DSS-induced oxidative stress primarily through the activation of PPARγ.

Oroxyloside inhibited ER stress in colitis mice via PPARγ activation

Previous studies have established that the accumulation of ROS can lead to protein damage, which in turn triggers the ER stress response [42]. To explore whether oroxyloside impacts ER stress, we evaluated the protein expression associated with ER stress through IHC, Western blotting assay, and immunofluorescence confocal microscopy. The results revealed that oroxyloside effectively inhibited the ER stress-associated signaling pathway, specifically the PERK-ATF4-CHOP pathway, including the components p-PERK, eIF2α, ATF4, and CHOP (Figs. 5A, 5B, and 5D). Additionally, real-time PCR results confirmed oroxyloside's similar inhibitory effects on the mRNA levels of sXBP-1 and CHOP (Fig. 5C). These analyses collectively demonstrate that oroxyloside mitigates DSS-induced ER stress. However, the inhibitory effect of oroxyloside on ER stress was significantly reversed by GW9662 (Figs. 5A–5D).

Oroxyloside decreased the production of pro-inflammatory cytokines via PPARγ activation in vitro

To determine whether PPARγ plays an important role in the anti-inflammatory effect of oroxyloside *in vitro*, we investigated the secretion of pro-inflammatory cytokines, including IL-1β, IL-6, and TNF-α in the RAW264.7 cell line and BMDM. Oroxyloside obviously inhibited LPS-induced production and transcription of these pro-inflammatory cytokines (Fig. 6A). Furthermore, silencing PPARγ by siRNA

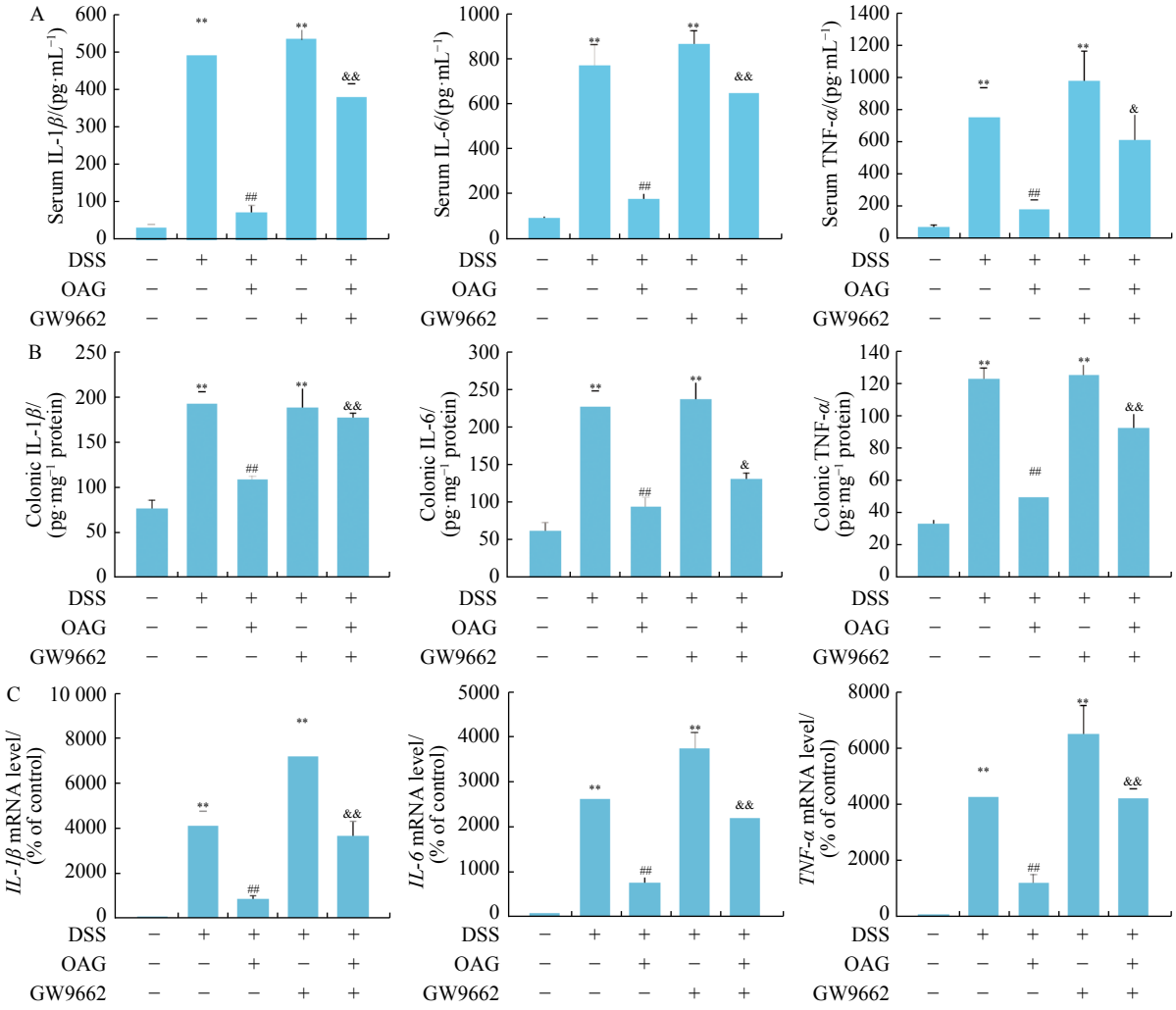

Fig. 3 Oroxyloside inhibited the production of pro-inflammatory cytokines *via* PPARγ activation in DSS-induced colitis mice. (A) The production of pro-inflammatory cytokines, IL-1β, IL-6, and TNF-α, in the serum and (B) in the colon were determined by ELISA in triplicate (n = 3 per group). (C) The mRNA levels of *IL-1β*, *IL-6*, and *TNF-α* were measured by real-time PCR (n = 3 per group). The results are expressed as means ± SD. $^{**}P < 0.01$ *vs* normal mice; $^{\#\#}P < 0.01$ *vs* DSS-treated colitis mice and $^{\&}P < 0.05$, $^{\&\&}P < 0.01$ *vs* DSS + OAG-treated colitis mice.

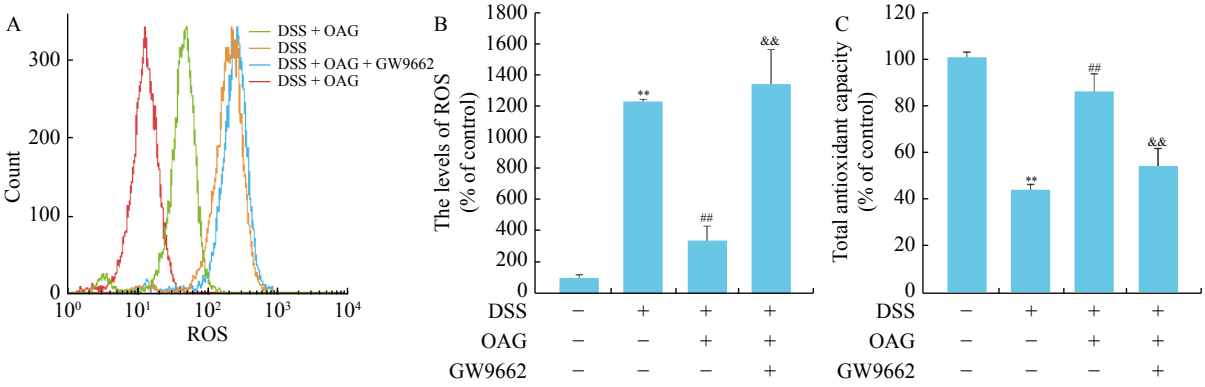

Fig. 4 Oroxyloside enhanced the antioxidant defenses by PPARγ activation in colitis mice. (A) The colonic tissue cells were incubated with DCFH/DA. The geometric mean DCF fluorescence was measured by flow cytometry. (B) Histograms represented the geometric mean DCF fluorescence (n = 3 per group). (C) The level of total antioxidant capacity was measured in colonic tissues (n = 3 per group). The results are expressed as means ± SD. $^{**}P < 0.01$ *vs* normal mice; $^{\#\#}P < 0.01$ *vs* DSS-treated colitis mice and $^{\&\&}P < 0.01$ *vs* DSS + OAG-treated colitis mice.

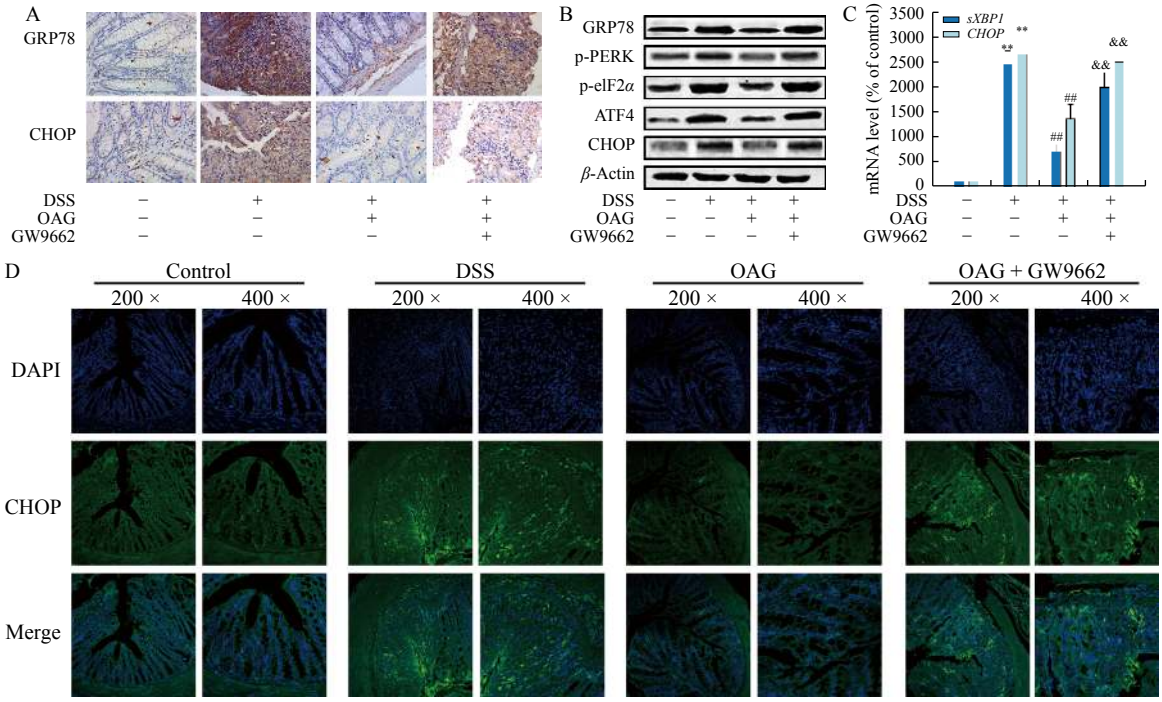

Fig. 5 Oroxyloside attenuated ER stress *via* PPARγ activation. (A) The levels of GRP78 and CHOP were assessed by IHC (×400) in colonic tissues. (B) The protein expression of GRP78, p-PERK, p-eIF2*α*, ATF4, CHOP, and *β*-actin were determined by Western blotting assay. *β*-Actin was used as a cytoplasm marker. (C) The mRNA levels of *sXBP1* and *CHOP* were measured by real-time PCR ($n = 3$ per group). (D) Immunofluorescence staining was detected to determine the effect of oroxyloside on the expression of CHOP in colonic tissues (200 ×). The results are expressed as means ± SD. $^{**}P < 0.01$ *vs* normal mice; $^{\#\#}P < 0.01$ *vs* DSS-treated colitis mice and $^{\&\&}P < 0.01$ *vs* DSS + OAG-treated colitis mice.

significantly increased the secretion of these cytokines, even in the presence of oroxyloside treatment (Fig. 6A). The results further demonstrated that PPARγ silencing negated the reduction of pro-inflammatory cytokines by oroxyloside at both the protein and mRNA levels in both RAW264.7 cells and BMDM (Figs. 6B and 6C). These findings collectively suggest that oroxyloside likely mitigates the production of pro-inflammatory cytokines through the activation of PPARγ.

Oroxyloside inhibited ER stress through PPARγ activation in vitro

In further investigations, we discovered that silencing PPARγ also blocked the inhibitory effect of oroxyloside on ROS generation *in vitro* (Figs. 7A and 7B). Our results showed that oroxyloside mitigated ER stress in the RAW264.7 cell line by decreasing the expression of key proteins involved in the PERK pathway, namely GRP78, p-PERK, and CHOP (Figs. 7C and 7D). Furthermore, oroxyloside was observed to reduce the increased protein levels of GRP78 and CHOP, while the effects were reversed by PPARγ silencing (Figs. 7E and 7F). Our data demonstrate that oroxyloside inhibited ER stress *via* PPARγ activation.

Discussion

With UC becoming increasingly prevalent in both developed and developing countries, addressing it has become an urgent need[2, 43]. UC is mainly characterized by intestinal inflammation and epithelial injury [44, 45]. The DSS-induced colitis model, which closely mimics human inflammatory bowel disease, offers a valuable tool for research [46]. Utilizing this model, our study investigated the anti-inflammatory effects of oroxyloside. We found that oroxyloside effectively countered DSS-induced colon length shortening and body weight loss (Fig. 1). Additionally, oroxyloside mitigated colonic pathological damage and the infiltration of inflammatory cells in mice with colitis (Fig. 2). As a nuclear receptor, PPARγ is a member of the PPAR family, which also includes PPARα and PPARβ/δ [47]. Expressed in a variety of cells within mucosal barriers, such as epithelial cells, lymphocytes, and monocytes/macrophages, PPARγ plays a crucial role in regulating numerous functions, including cell proliferation, epithelial integrity, and mucosal bacterial-induced inflammation [48, 49]. Intriguingly, the anti-inflammatory effects of oroxyloside were reversed by the PPARγ inhibitor GW9662 (Figs. 1 and 2), suggesting that oroxyloside exerts its protective effects against DSS-induced colitis primarily through the activation of PPARγ.

Cytokines play a crucial role in controlling intestinal inflammation and have been directly implicated in the pathogenesis of IBD in current genetic and immunological studies [50]. In this study, the results demonstrated that oroxyloside effectively ameliorated colitis by reducing the elevated levels of pro-inflammatory cytokines IL-1β, IL-6, and TNF-α in the serum and colon of mice with DSS-induced colitis (Fig. 3). However, GW9662 blocked the inhibitory effects of

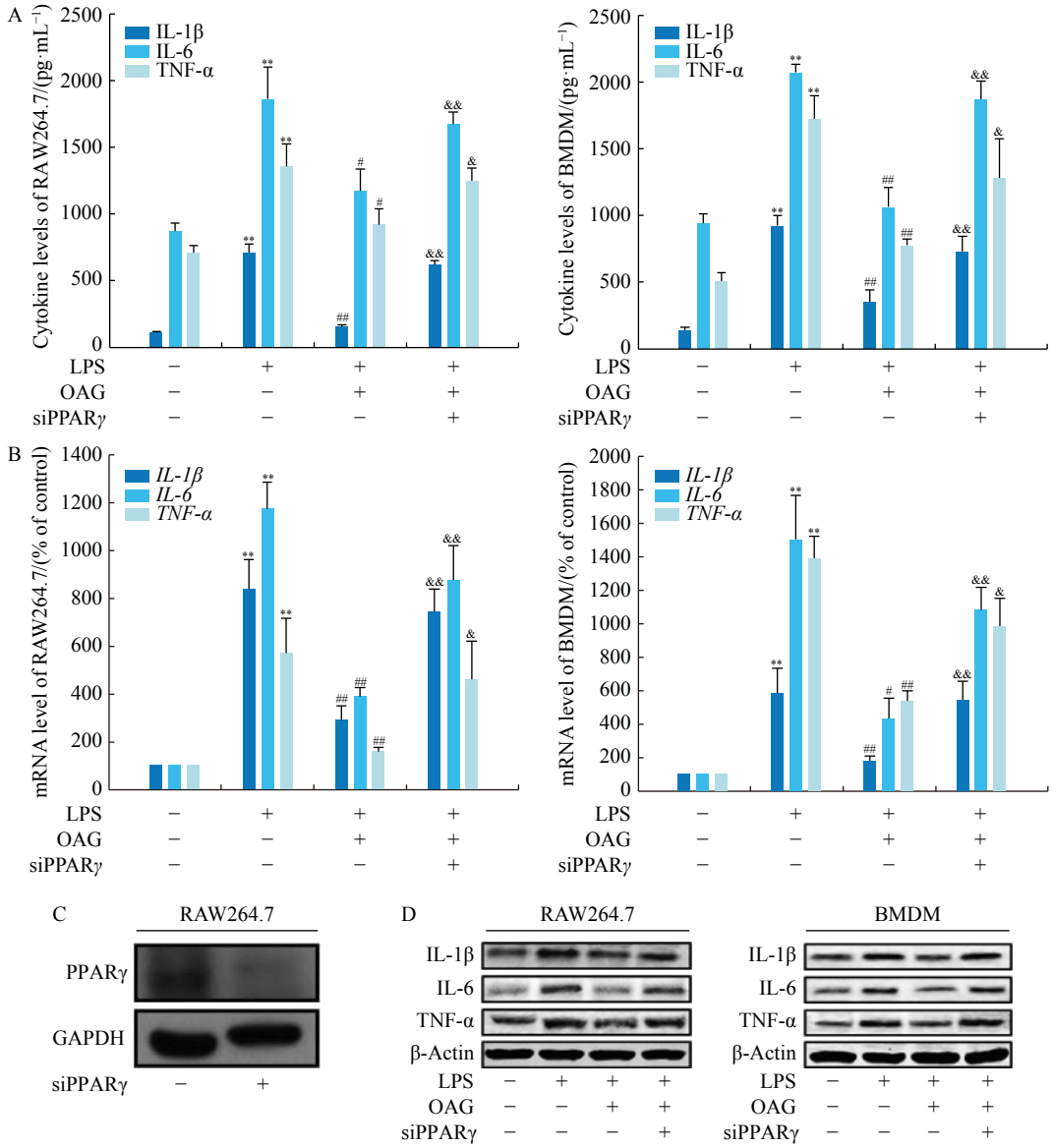

Fig. 6 Oroxyloside reduced the production of pro-inflammatory cytokines by PPARγ activation *in vitro*. (A) IL-1β, IL-6, and TNF-α in culture supernatants were measured by ELISA in RAW 264.7 cells and BMDM (n = 3 per group). (B) The mRNA levels of *IL-1β*, *IL-6*, and *TNF-α* were measured by real-time PCR in RAW 264.7 cells and BMDM (n = 3 per group). (C, D) The protein expressions of PPARγ, IL-1β, IL-6, and TNF-α were assessed by Western blotting assay. The results are expressed as means ± SD. $^{**}P < 0.01$ *vs* control; $^{\#}P < 0.05$, $^{\#\#}P < 0.01$ *vs* LPS-treated group and $^{\&}P < 0.05$, $^{\&\&}P < 0.01$ *vs* LPS + OAG-treated group.

oroxyloside on the pro-inflammatory cytokines. In the serum, the levels of all three cytokines (IL-1β, IL-6, and TNF-α) in the DSS + OAG + GW9662 group were nearly tripled compared to the DSS + OAG group. These findings indicated that oroxyloside inhibited the production of pro-inflammatory cytokines in DSS-induced colitis *via* PPARγ activation.

Over the past few decades, ROS has been increasingly recognized as a potential etiological factor in the pathogenesis of intestinal damage in IBD [51]. Our study further demonstrated that oroxyloside (80 mg·kg^{-1} *in vivo*, 100 μmol·L^{-1} *in vitro*) decreased the ROS generation induced by DSS in mice or LPS in macrophage, respectively (Figs. 4A, 4B and Figs. 7A, 7B). GW9662 and PPARγ siRNA also reversed the inhibitory effects of oroxyloside on ROS generation *in vivo* and *in vitro* (Figs. 4A, 4B and Figs. 7A, 7B). In the i*n vivo* study, the ROS production of the DSS + OAG + GW9662 group was more than three times to the DSS + OAG group, and a similar phenomenon was shown in the *in vitro* study as well. The results indicated that oroxyloside inhibited the generation of ROS *via* PPARγ activation.

The accumulation of ROS leads to ER stress, which arises from the excessive presence of misfolded or unfolded proteins in the ER, triggering the UPR [52, 53]. The UPR is regulated by three major pathways and their associated transcription factors: PERK-ATF4, ATF6p90-ATF6p50, and IRE1-XBP1 [53]. Genetic correlations between ER stress and both

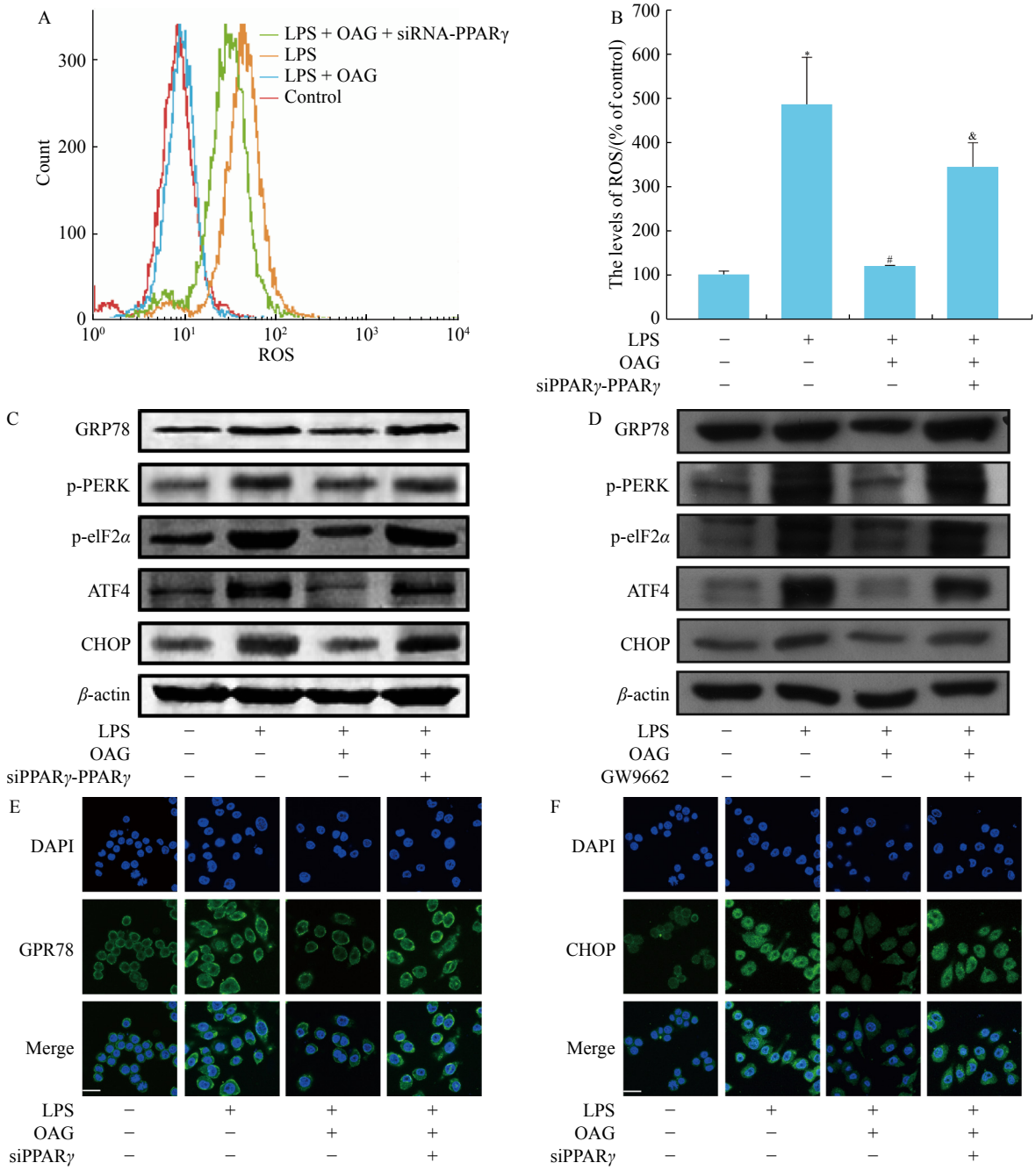

Fig. 7 Oroxyloside inhibited ER stress through PPARγ activation *in vitro*. (A) RAW264.7 cells were incubated with DCFH/DA. The geometric mean DCF fluorescence was measured by flow cytometry. (B) Histograms represented the geometric mean DCF fluorescence (n = 3 per group). (C, D) The protein expressions of GRP78, p-PERK, p-eIF2α, ATF4, CHOP, and β-actin were determined by Western blotting assay. β-Actin was used as a cytoplasm marker. (E, F) Immunofluorescence staining was detected to determine the effect of oroxyloside on the expression of GRP78 and CHOP in RAW264.7 cells (200 ×). The results are expressed as means ± SD. $^{*}P < 0.05$ *vs* control; $^{\#}P < 0.05$ *vs* LPS-treated group and $^{\&}P < 0.05$ *vs* LPS + OAG-treated group.

forms of IBD, CD, and UC, have been identified, initially through a candidate gene study of *XBP1* [18] and more recently *via* the GWAS-based identification of the ORMDL3 locus [54]. During ROS-induced ER stress, the PERK-ATF4-CHOP pathway is a key signaling cascade [55-58]. However, it remains unclear whether CHOP is activated specifically through ROS-triggered ER stress in UC. In our study, treatment with DSS (*in vivo*) or LPS (*in vitro*) elevated the protein levels of canonical UPR genes such as *GRP78* compared with control groups. Furthermore, activation of PERK pathway components, evidenced by increased protein expression of *CHOP* (also known as *DDIT3*) and *ATF4*, was observed in colitis tissue (DSS-induced) or macrophages (post-LPS treatment) compared with their respective control groups (Figs. 5B and 7C). To reinforce these findings, we also validated the protein expression of CHOP through immunofluorescence

confocal microscopy (Figs. 5D and 7E). The influence of oroxyloside on ER stress was negated by silencing PPARγ (Figs. 7C–7E); there are literature reports that oroxyloside could directly activate PPARγ [59-61]. Our data suggest that oroxyloside mitigates ER stress induced by ROS through the activation of PPARγ.

In conclusion, oroxyloside inhibits DSS-induced colonic pathological damage, inflammatory cell infiltration, activity of MPO, and the generation of ROS. The pro-inflammatory cytokines in the serum and colon were also significantly reduced by oroxyloside. Furthermore, we illuminated that oroxyloside protected against DSS-induced colitis by suppressing ER stress through PPARγ activation. These outcomes were corroborated by our *in vitro* experiments in the mouse macrophage cell line RAW264.7 and BMDM, providing pivotal insights into the mechanism by which oroxyloside restores the compromised antioxidant defense, thereby alleviating DSS-induced colitis. Furthermore, this study suggests that oroxyloside might be a promising candidate for the treatment of IBD.

References

[1] Lakatos PL. Recent trends in the epidemiology of inflammatory bowel diseases: up or down? [J]. *World J Gastroenterol*, 2006, **12**(38): 6102-6108.

[2] Edward V Loftus Jr. Clinical epidemiology of inflammatory bowel disease: Incidence, prevalence, and environmental influences [J]. *Gastroenterology*, 2004, **126**(6): 1504-1517.

[3] Satsangi J, Silverberg MS, Vermeire ES, *et al*. The Montreal classification of inflammatory bowel disease: controversies, consensus, and implications [J]. *Gut*, 2006, **55**(6): 749-753.

[4] Bertolotti A, Wang X, Novoa I, *et al*. Increased sensitivity to dextran sodium sulfate colitis in IRE1beta-deficient mice [J]. *J Clin Invest*, 2001, **107**(5): 585-593.

[5] Cao SS, Zimmermann EM, Chuang BM, *et al*. The unfolded protein response and chemical chaperones reduce protein misfolding and colitis in mice [J]. *Gastroenterology*, 2013, **144**(5): 989-1000.e6.

[6] Rutkowski T, Kaufman RJ. A trip to the ER: coping with stress [J]. *Trends Cell Biol*, 2004, **14**(1): 20-28.

[7] Walter P, Ron D. The unfolded protein response: from stress pathway to homeostatic regulation [J]. *Science*, 2011, **334**(6059): 1081-1086.

[8] Rutkowski DT, Arnold SM, Miller CN, *et al*. Adaptation to ER stress is mediated by differential stabilities of pro-survival and pro-apoptotic mRNAs and proteins [J]. *PLoS Biol*, 2006, **4**(11): e374.

[9] Zinszner H, Kuroda M, Wang X, *et al*. CHOP is implicated in programmed cell death in response to impaired function of the endoplasmic reticulum [J]. *Genes Dev*, 1998, **12**(7): 982-995.

[10] Oyadomari S, Koizumi A, Takeda K, *et al*. Targeted disruption of the Chop gene delays endoplasmic reticulum stress-mediated diabetes [J]. *J Clin Invest*, 2002, **109**(4): 525-532.

[11] Feng B, Yao PM, Li Y, *et al*. The endoplasmic reticulum is the site of cholesterol-induced cytotoxicity in macrophages [J]. *Nat Cell Biol*, 2003, **5**(9): 781-792.

[12] Song B, Scheuner D, Ron D, *et al*. Chop deletion reduces oxidative stress, improves beta cell function, and promotes cell survival in multiple mouse models of diabetes [J]. *J Clin Invest*, 2008, **118**(10): 3378-3389.

[13] Lin JH, Li H, Yasumura D, *et al*. IRE1 signaling affects cell fate during the unfolded protein response [J]. *Science*, 2007, **318**(5852): 944-949.

[14] Thorp E, Li G, Seimon TA, *et al*. Reduced apoptosis and plaque necrosis in advanced atherosclerotic lesions of Apoe$^{-/-}$ and Ldlr$^{-/-}$ mice lacking CHOP [J]. *Cell Metab*, 2009, **9**(5): 474-481.

[15] Shkoda A, Ruiz PA, Daniel H, *et al*. Interleukin-10 blocked endoplasmic reticulum stress in intestinal epithelial cells: impact on chronic inflammation [J]. *Gastroenterology*, 2007, **132**(1): 190-207.

[16] Hu S, Ciancio MJ, Lahav M, *et al*. Translational inhibition of colonic epithelial heat shock proteins by IFN-gamma and TNF-alpha in intestinal inflammation [J]. *Gastroenterology*, 2007, **133**(6): 1893-1904.

[17] Heazlewood CK, Cook MC, Eri R, *et al*. Aberrant mucin assembly in mice causes endoplasmic reticulum stress and spontaneous inflammation resembling ulcerative colitis [J]. *PLoS Med*, 2008, **5**(3): e54.

[18] Kaser A, Lee AH, Frankea A, *et al*. XBP1 links ER stress to intestinal inflammation and confers genetic risk for human inflammatory bowel disease [J]. *Cell*, 2008, **134**(5): 743-756.

[19] Desreumaux P, Dubuquoy L, Nutten S, *et al*. Attenuation of colon inflammation through activators of the retinoid X receptor (RXR)/peroxisome proliferator-activated receptor gamma (PPARgamma) heterodimer. A basis for new therapeutic strategies [J]. *J Exp Med*, 2001, **193**(7): 827-38.

[20] NakajimaA A, Wada K, Miki H, *et al*. Endogenous PPAR gamma mediates anti-inflammatory activity in murine ischemia-reperfusion injury [J]. *Gastroenterology*, 2001, **120**(2): 460-469.

[21] Su CG, Wen X, Bailey ST, *et al*. A novel therapy for colitis utilizing PPAR-gamma ligands to inhibit the epithelial inflammatory response [J]. *J Clin Invest*, 1999, **104**(4): 383-389.

[22] Gold PW, Licinio J, Pavlatou MG. Pathological parainflammation and endoplasmic reticulum stress in depression: potential translational targets through the CNS insulin, klotho and PPAR-gamma systems [J]. *Mol Psychiatry*, 2013, **18**(2): 154-165.

[23] Ikeda J, Ichiki T, Takahara Y, *et al*. PPARgamma agonists attenuate palmitate-induced ER stress through up-regulation of SCD-1 in macrophages [J]. *PLoS One*, 2015, **10**(6): e0128546.

[24] Takahashi N, Yoshizaki T, Hiranaka N, *et al*. Endoplasmic reticulum stress suppresses lipin-1 expression in 3T3-L1 adipocytes [J]. *Biochem Biophys Res Commun*, 2013, **431**(1): 25-30.

[25] Ren Y, Sun C, Sun Y, *et al*. PPAR gamma protects cardiomyocytes against oxidative stress and apoptosis *via* Bcl-2 upregulation [J]. *Vascul Pharmacol*, 2009, **51**(2-3): 169-174.

[26] Aoun P, Simpkins JW, Agarwal N. Role of PPAR-gamma ligands in neuroprotection against glutamate-induced cytotoxicity in retinal ganglion cells [J]. *Invest Ophthalmol Vis Sci*, 2003, **44**(7): 2999-3004.

[27] Bordet R, Ouk T, Petrault O, *et al*. PPAR: a new pharmacological target for neuroprotection in stroke and neurodegenerative diseases [J]. *Biochem Soc Trans*, 2006, **34**(Pt 6): 1341-6.

[28] Yi JH, Park SW, Kapadia R, *et al*. Role of transcription factors in mediating post-ischemic cerebral inflammation and brain damage [J]. *Neurochem Int*, 2007, **50**(7-8): 1014-1027.

[29] Tureyen K, Kapadia R, Owen KK, *et al*. Peroxisome proliferator-activated receptor-gamma agonists induce neuroprotection following transient focal ischemia in normotensive, normoglycemic as well as hypertensive and type-2 diabetic rodents [J]. *J Neurochem*, 2007, **101**(1): 41-56.

[30] Sun Y, Lu N, Ling Y, *et al*. Oroxylin A suppresses invasion through down-regulating the expression of matrix metalloproteinase-2/9 in MDA-MB-435 human breast cancer cells [J]. *Eur J Pharmacol*, 2009, **603**(1-3): 22-28.

[31] Li HN, Nie FF, Liu W, *et al*. Apoptosis induction of oroxylin A in human cervical cancer HeLa cell line *in vitro* and *in vivo* [J]. *Toxicology*, 2009, **257**(1-2): 80-85.
[32] Wang X, Sun Y, Zhao Y, *et al*. Oroxyloside prevents dextran sulfate sodium-induced experimental colitis in mice by inhibiting NF-κB pathway through PPARγ activation [J]. *Biochem Pharmacol*, 2016, **106**: 70-81.
[33] Yao J, Pan D, Zhao Y, *et al*. Wogonin prevents lipopolysaccharide-induced acute lung injury and inflammation in mice *via* peroxisome proliferator-activated receptor gamma-mediated attenuation of the nuclear factor-kappaB pathway [J]. *Immunology*, 2014, **143**(2): 241-257.
[34] Mu R, Qi Q, Gu H, *et al*. Involvement of p53 in oroxylin A-induced apoptosis in cancer cells [J]. *Mol Carcinog*, 2009, **48**(12): 1159-1169.
[35] Zhao Y, Yao J, Wu XP, *et al*. Wogonin suppresses human alveolar adenocarcinoma cell A549 migration in inflammatory microenvironment by modulating the IL-6/STAT3 signaling pathway [J]. *Mol Carcinog*, 2015, **54**(Suppl 1): E81-E93.
[36] Zhao Y, Yao J, Wu X P, *et al*. Wogonin suppresses human alveolar adenocarcinoma cell A549 migration in inflammatory microenvironment by modulating the IL-6/STAT3 signaling pathway [J]. *Mol Carcinog*, 2014, **54**(S1): E81-E93.
[37] Okayasu I, Hatakeyama S, Yamada M, *et al*. A novel method in the induction of reliable experimental acute and chronic ulcerative colitis in mice [J]. *Gastroenterology*, 1990, **98**(3): 694-702.
[38] Hickey MJ. MPO and neutrophils: a magnetic attraction [J]. *Blood*, 2011, **117**(4): 1103-1104.
[39] Reumaux D, De Boer M, Meijer AB, *et al*. Expression of myeloperoxidase (MPO) by neutrophils is necessary for their activation by anti-neutrophil cytoplasm autoantibodies (ANCA) against MPO [J]. *J Leukoc Biol*, 2003, **73**(6): 841-849.
[40] Egger B, Bajaj-Elliott M, Macdonald TT, *et al*. Characterisation of acute murine dextran sodium sulphate colitis: cytokine profile and dose dependency [J]. *Digestion*, 2000, **62**(4): 240-248.
[41] Garside P. Cytokines in experimental colitis [J]. *Clin Exp Immunol*, 1999, **118**(3): 337-339.
[42] Araki Y, Andoh A, Fujiyama Y. The free radical scavenger edaravone suppresses experimental dextran sulfate sodium-induced colitis in rats [J]. *Int J Mol Med*, 2003, **12**(1): 125-129.
[43] Clarke HJ, Chambers JE, Liniker E, *et al*. Endoplasmic reticulum stress in malignancy [J]. *Cancer Cell*, 2014, **25**(5): 563-573.
[44] Mohamadzadeh M, Pfeiler EA, Brown JB, *et al*. Regulation of induced colonic inflammation by *Lactobacillus acidophilus* deficient in lipoteichoic acid [J]. *Proc Natl Acad Sci USA*, 2011, **108**(Suppl 1): 4623-4630.
[45] Danese S, Fiocchi C. Ulcerative colitis [J]. *N Engl J Med*, 2011, **365**(18): 1713-1725.
[46] Baumgart DC, Sandborn WJ. Crohn's disease [J]. *Lancet*, 2012, **380**(9853): 1590-605.
[47] Perse M, Cerar A. Dextran sodium sulphate colitis mouse model: traps and tricks [J]. *J Biomed Biotechnol*, 2012, **2012**: 718617.
[48] Feige JN, Gelman L, Michalik L, *et al*. From molecular action to physiological outputs: peroxisome proliferator-activated receptors are nuclear receptors at the crossroads of key cellular functions [J]. *Prog Lipid Res*, 2006, **45**(2): 120-159.
[49] Lefebvre M, Paulweber B, Fajas L, *et al*. Peroxisome proliferator-activated receptor gamma is induced during differentiation of colon epithelium cells [J]. *J Endocrinol*, 1999, **162**(3): 331-340.
[50] Katayama K, Wada K, Nakajima A, *et al*. A novel PPAR gamma gene therapy to control inflammation associated with inflammatory bowel disease in a murine model [J]. *Gastroenterology*, 2003, **124**(5): 1315-1324.
[51] StroberR W, Fuss IJ, Blumberg RS. The immunology of mucosal models of inflammation [J]. *Annu Rev Immunol*, 2002, **20**: 495-549.
[52] Oz HS, Chen TS, Mcclain CJ, *et al*. Antioxidants as novel therapy in a murine model of colitis [J]. *J Nutr Biochem*, 2005, **16**(5): 297-304.
[53] Todd DJ, Lee AH, Glimcher LH. The endoplasmic reticulum stress response in immunity and autoimmunity [J]. *Nat Rev Immunol*, 2008, **8**(9): 663-74.
[54] Schroder M, Kaufman RJ. The mammalian unfolded protein response [J]. *Annu Rev Biochem*, 2005, **74**: 739-789.
[55] Winnay JN, Boucher J, Mori MA, *et al*. A regulatory subunit of phosphoinositide 3-kinase increases the nuclear accumulation of X-box-binding protein-1 to modulate the unfolded protein response [J]. *Nat Med*, 2010, **16**(4): 438-445.
[56] Takahashi A, Masuda A, Sun M, *et al*. Oxidative stress-induced apoptosis is associated with alterations in mitochondrial caspase activity and Bcl-2-dependent alterations in mitochondrial pH (pHm) [J]. *Brain Res Bull*, 2004, **62**(6): 497-504.
[57] Heta C, Bernasconi P, Fisher J, *et al*. Proapoptotic BAX and BAK modulate the unfolded protein response by a direct interaction with IRE1alpha [J]. *Science*, 2006, **312**(5773): 572-576.
[58] Martin-Perez R, Palacios C, Yerbes R, *et al*. Activated ERBB2/HER2 licenses sensitivity to apoptosis upon endoplasmic reticulum stress through a PERK-dependent pathway [J]. *Cancer Res*, 2014, **74**(6): 1766-1777.
[59] Trachootham D, Alexandre J, Huang P. Targeting cancer cells by ROS-mediated mechanisms: a radical therapeutic approach? [J]. *Nat Rev Drug Discov*, 2009, **8**(7): 579-591.
[60] Zhou Y, Guo Y, Zhu Y, *et al*. Dual PPARγ/α agonist oroxyloside suppresses cell cycle progression by glycolipid metabolism switch-mediated increase of reactive oxygen species levels [J]. *Free Radical Biol Med*, 2021, **167**: 205-217.
[61] Tang Y, Wei K, Liu L, *et al*. Activation of PPARγ protects obese mice from acute lung injury by inhibiting endoplasmic reticulum stress and promoting mitochondrial biogenesis [J]. *PPAR Re*, 2022, **2022**: 7888937.

Cite this article as: TAO Lei, DOU Renjie, CHEN Xueming, CAO Yu, DAI Zhen, HU Ziyan, MA Zhi, GE Xiaoming, ZHANG Ling, WANG Xiaoping. Oroxyloside protects against dextran sulfate sodium-induced colitis by inhibiting ER stress *via* PPARγ activation [J]. *Chin J Nat Med*, 2024, **22**(4): 307-317.